Functionalization of Peptide-coated Platinum Nanoparticles for Various Biological Applications

Michal S. Shoshan,[a] Mao Li,[a] Thomas Vonderach,[b] and Helma Wennemers[a]*

Functionalizing noble metal nanoparticles is often necessary to tailor their properties, in particular for biological applications such as drug delivery, therapy and imaging. However, this process is highly challenging, due to the complications in maintaining similar geometrical parameters of the nanoparticles as of without functionalization. The heptapeptide H-Lys-[Pro-Gly-Lys]$_2$-NH$_2$ was found to be an efficient additive for the formation and stabilization of small and monodisperse platinum nanoparticles (PtNPs). We show that the same additive peptide can be used as a platform for the functionalization of PtNPs, as demonstrated by the introducion of three different moieties: coumarin for monitoring cellular uptake of the PtNPs; biotin for detecting their stability in human blood serum; and an arginine-containing peptide for enhanced cell penetration. The peptide-coated PtNPs can be functionalized both before and after reduction of the metal ions, in aqueus environment, emphasizing the high robustness of the system.

Introduction

Peptides are attractive additives for the formation and stabilization of noble metal nanoparticles (NPs).[1-4] Such peptide-coated NPs have been applied for *e.g.* drug delivery, therapy, imaging, and catalysis.[5-7] For many of these applications, functionalization of the nanoparticles is necessary to enhance their cellular uptake, targeting, selectivity, imaging, *etc*.[8-10] However, functionalization, either before or after nanoparticle formation, can lead to NP aggregation or to other morphological changes and is therefore a challenging process.[10] Noble metal NP are formed by reducing the corresponding metal ions in the presence of an additive that enables to control the size and shape of the NPs and serves as a shell around the metal core.

The functionalization can be achieved by (a) the attachment of the functional moiety to the additive before NP formation (pre-reductive functionalization), or (b) ligation of the functioned moiety, after NP formation.[10] Both strategies have advantages and drawbacks: functionalization of the additive before NP formation enables to control the ratio between the functionalized moieties and the additive. In addition, it saves an additional synthetic step and does not require examining the presence of the functional moiety. Post-reductive functionalization is a preferred approach in several cases such as the instability of the functionalized moiety toward the reductive conditions that are required for NP formation,[10, 11] or in case the required functionality interferes with the NP formation and destabilizes them.[10] However, post-reductive functionalization also suffer from several drawbacks, mainly related to relatively low conversion and difficulties in identifying the functionalization success.[10, 12] In addition, in both cases the NP formation as well as the functionalization take place in an organic environment and a solvent replacement is crucial for further application.

We have recently introduced the peptide H-Lys-[Pro-Gly-Lys]$_2$-NH$_2$ (**1**) as an additive for the formation of platinum nanoparticles (PtNPs) with a narrow size distribution of 2.5 ± 0.7 nm that are stable for more than a year.[13] These PtNPs are toxic against hepatocellular carcinoma (HCC) cells HepG2, whereas they barely affect the viability of other cell-lines.[13]

Structure activity relationship (SAR) studies revealed that the amino groups in the peptide are essential for the formation and stabilization of the PtNPs and can therefore not be replaced or further functionalized.[13] Also the sequence of Lys in the i, i+3 positions was found to be crucial and the C-terminal must be capped. However, the residues between the Lys can be replaced without harming the formation of the PtNPs.[13] Attachment of glucose to the Cγ of Pro2[14] enabled to enhance cellular uptake and cytotoxicity.[13] We therefore envisioned that the Cγ of Pro can be relatively easy and straightforward functionalized, in order to expand the applicability of the PtNPs.

Herein, we probed whether peptide **1** can be functionalized by different moieties that would allow for fluorescent imaging of the PtNPs inside the cells, PtNP recovery, and enhanced cell penetration of the peptide-PtNP conjugates. We show that in three different cases, the functionalization of the peptidic ligand undergoes in an aqueous environment and does not interfere with the formation and stabilization of the PtNPs. The functionalized PtNPs have similar sizes and shelf-lives, as the non-functionalized PtNPs. Furthermore, we demonstrate that peptide **1** can be functionalized both before and after PtNP formation, by the Staudinger ligation.[15] These examples highlight the robustness of peptide-coated PtNPs and emphasize its great potential toward a variety of functional moieties.

Results and Discussion

Synthesis of functionalized peptides for PtNP formation

We started by testing which type of functional moieties that are attached to **1** still allow for NP formation. Specifically, we were interested in different analogues of **1** with several biologically relevant moieties at the side chain of the second position: (a) coumarin for the fluorescent identification of cellular uptake (**1a**), (b) biotin for the determination of NP stability in human blood serum (**1b**), (c) two guanidinium-containing peptides for enhanced cell penetration (**1c** and **1d** with arginine (R) and *4S*-guanidiniumproline[16] (Z, Gup), respectively).[17-19] In addition,

synthesized another analogue with an azido group as a functionalization site (**1e**) for post-reductive functionalization. Coumarin was chosen as it is a neutral moiety that should not compete with the peptide for binding to the metal surface. Similarly in case of biotin, it is not expected to interact with the bulk NP. Peptides **1c** and **1d** are expected to increase cellular uptake but also may undesirably compete with Lys side chains in binding the nanoparticle surface.

Peptides **1a**-**1e** were synthesized by standard Fmoc-based solid-phase peptide synthesis (SPPS) on Rink amide resin (Scheme 1).[13] The (4*S*)Azidoproline ((4*S*)Azp) in the second position of the resin-bound precursor was reduced by Staudinger reduction, followed by coupling of carboxylic acid derivatives of coumarin (**1a**) and biotin (**1b**), respectively, to the newly formed amine. Boc-Lys(Boc) was introduced at the N-terminal position, as Fmoc is unstable towards the conditions of Staudinger reduction. Peptides **1c** and **1d** were synthesized by SPPS in similar conditions, introducing Fmoc-Arg(Pbf)-OH or Fmoc-Gup(Boc)$_2$-OH, respectively. After cleavage from the solid support, the peptides were purified by HPLC and desalted, to achieve the desired additive analogues **1a**-**1e**.

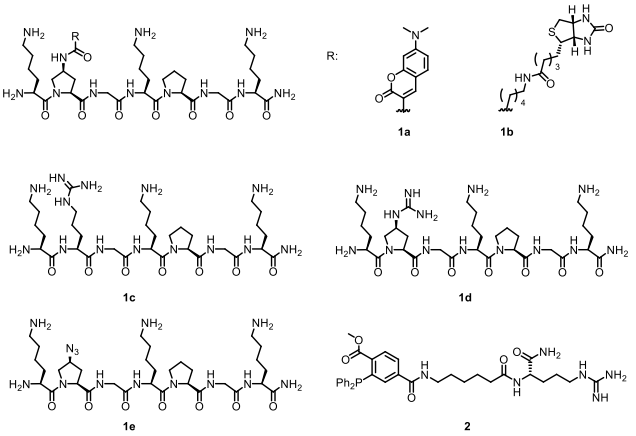

Scheme 1. Structure of peptides **1a**-**1e** and **2**.

In addition, to investigate the potential of peptides for post-reductive functionalization, we synthesized **2** (Scheme 1). This peptide contains arginine attached to a triphenylphosphine moiety (with aminohexanoic acid as a linker) for post-reductive functionalization, that was synthesized using standard Fmoc-based SPPS on Rink amide resin, where at the third coupling 3-(diphenylphosphaneyl)-4-(methoxycarbonyl)benzoic acid[20] was introduced.

Synthesis of functionalized PtNPs

Next we explored whether peptides **1a**-**1e** can form stable, small and monodisperse PtNPs, similarly to peptide **1**. We therefore synthesized the PtNPs following a previously established protocol[13] and were analyzed by transmission electron microscope (TEM) and ζ potential (Table 1; Figure 1).

Table 1. Properties of PtNPs formed in the presence of analogues of **1**

Entry	Peptide	Additional functionalization	Diameter[a] (nm)	ζ potential (mV)
1	**1**[13]	-	2.5 ± 0.7	3.6 ± 0.8
2	**1Glc**[13]	Glucose	2.7 ± 0.8	2.5 ± 1.2
3	**1a**	Coumarin	1.9 ± 0.4	2.9 ± 0.5
4	**1b**	Biotin	1.8 ± 0.4	4.1 ± 1.0
5	**1c**	Arginine	Aggregation[b]	n.d.[d]
6	**1d**	Gup	Aggregation[b]	n.d.[d]
7	**1d**[c]	Gup	Aggregation[e]	n.d.[d]
8	**1e**	Azide	2.2 ± 0.5	3.1 ± 0.3
9	**1e2**	Post-Arg[f]	2.6 ± 0.8	14.7 ± 1.1

[a] After purification. [b] PtNPs aggregated in the crude mixture within hours. [c] In pH 13 (5 M KOH). [d] Not determined. [e] PtNPs aggregated after purification. [f] Post-reductive functionalization of Arg-containing tripeptide.

PtNP-**1a** and PtNP-**1b** (Table 1 entries 3 and 4, Figure 1) were found to be slightly smaller to the PtNPs bearing no additional functionality (Table 1 entry 1) or to the glucose decorated PtNPs (Table 1 entry 2). However, the dispersity and stability of the PtNPs, together with the error range of their sizes reflect their similarity to the previous PtNPs. This observation shows that neither coumarin nor biotin affect the geometrical characteristics of the PtNPs and that the ability of coumarin to form π stacked assemblies[21] and the bulkiness of both moieties did not influence PtNP assembly. In contrast, no stable PtNPs were obtained with peptides **1c** and **1d** as additives (Table 1 entries 5 and 6; Figure 1). Having a higher isoelectric point than peptide **1**, we suspected that an electrostatic repulsion between **1c** or **1d** and the Pt(II) ions prevents NP formation. To minimize this repulsion, we repeated the PtNP formation with **1d** at pH 13 instead of 9. However, the formed PtNPs coalesced upon purification (Table 1 entry 7; Figure 1). Thus the presence of a guanidinium group inhibits the formation of stable PtNPs either by the repulsion or by competing with Lys side chains on binding to the metal surface. We therefore explored whether post-reductive functionalization can be of use for the introduction of a guanidinium group to the surface of PtNPs.

For that purpose, PtNPs were formed in the presence of a peptide containing (*4S*)Azp (H-Lys-Azp-Gly-Lys-Pro-Gly-Lys-NH_2) instead of Pro at the second position (**1e**; Scheme 1; Table 1 entry 8). PtNP-**1e** were found to be stable upon dialysis, lyophilization and resuspension. To perform post-reductive functionalization of PtNP-**1e**, we chose the Staudinger-Bertozzi ligation as it does not involve any additional metal precursor and can easily be monitored by NMR. We synthesized the dipeptide H-Ahx-Arg-NH_2 which was functionalized on-resin with the triphenylphosphine motif (**2**; Scheme 1).[15, 20]

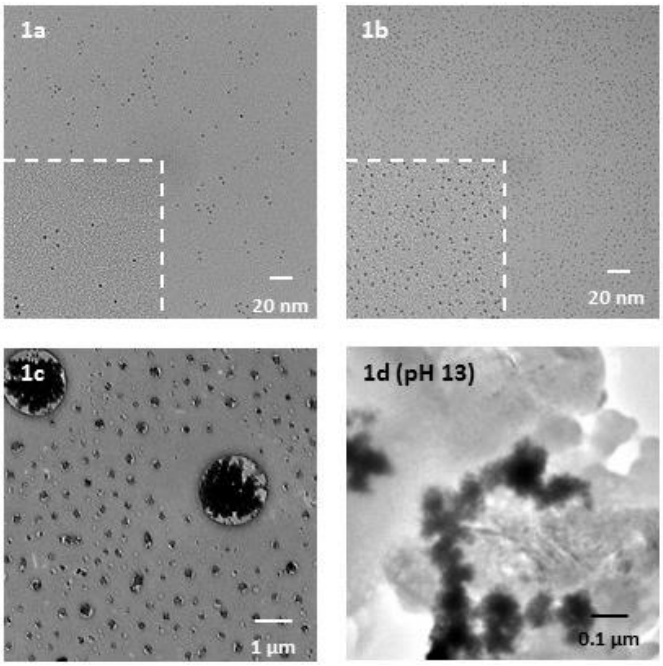

Figure 1. TEM micrographs of purified PtNP-**1a** and PtNP-**1b**. TEM micrographs of Pt aggregation, formed in the presence of **1c** and of **1d** (at pH 13).

The dialyzed PtNP-**1e** were then reacted with peptide **2** (1.5 eq.) for 48 h. We succeeded forming the post-reductive functionalized PtNP-**1e2** (Scheme 2) that were further purified by an additional dialysis step to remove traces of unreacted peptide **2**. The functionalization step was detected by ^{31}P NMR and ζ potential analyses of the suspension. The peak corresponding to triphenylphosphine moiety in the ^{31}P NMR, was shifted from -3.3 ppm to +34.4 ppm, which indicates the formation of oxidized phosphoxide (Figure S2). This result indicates that the Ahx-Arg fragment was incorporated with the peptide-coated PtNPs. In addition, ζ potential measurements showed a significant increase of the potential of PtNP-**1e2** compared to the value of PtNP-**1e**, from 3.1 ± 0.3 mV to 14.7 ± 1.1 mV, respectively. These differences indicate that the Arg is most likely solvent-exposed. We overcame the obstacles of introducing guanidinium groups on the surface of the PtNPs and formed PtNP-**1e2** that were found to be stable for more than 6 months in suspension as well as a powder, as shown by TEM.

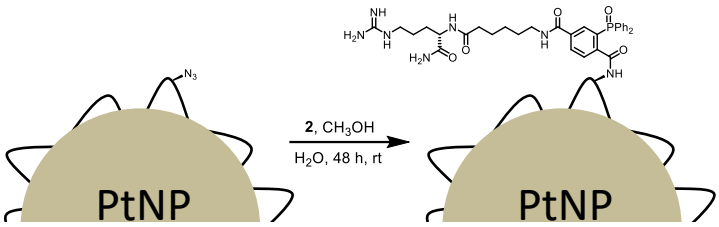

Scheme 2. Synthesis of PtNP-**1e2** using post-reductive Staudinger-Bertozzi ligation.

Applications of PtNPs

Determination of cellular uptake

Decoration of the PtNPs with a fluorophore allows to identify them in the cellular environment. In order to track after PtNP-**1a** in the cellular environment, we first investigated their effect on the cell viability of five representative cell-lines: cervical adenocarcinoma cells (HeLa), colon adenocarcinoma cells (HT-29), epidermoid carcinoma cells (A431), hepatocellular carcinoma cells (HepG2), and normal liver mouse cells (AML-12). These cell-lines were chosen based on previous results on the effect of PtNP-**1** and PtNP-**1Glc** on their cell-viability: the hepatocellular carcinoma cells HepG2 were dramatically affected by treatment with these PtNPs, but the rest of the cells, including the healthy liver cells AML-12, were barely affected.[13] Similarly to the previously investigated PtNPs, also PtNP-**1a** were found to be toxic only against HepG2 cell-line. However, the effect of PtNP-**1a** were found to be slightly smaller compared to the one of PtNP-**1**.[22] This observation might be related to a reduced cellular uptake of PtNP-**1a** compared to the non-fluorescent PtNPs, due to the coumarin. Nevertheless, we could now use PtNP-**1a** as an indicative system to our peptide-coated PtNPs.

To probe the PtNP intracellular location, PtNP-**1a** were incubated for 12 h[23] with the same five representative cell-lines, after their nuclei were labelled with red fluorescence protein. Upon extensive washing, the cells were further analyzed by confocal microscopy (Figure 2).

In all five cell-lines, accumulation of the PtNPs in the cytoplasm was observed. However, the fluorescence intensity in HepG2 cells was found to be higher than in the other four cell-lines. These differences also reflected by the higher cellular uptake compared to HT-29 cells that has been measured by inductively coupled plasma mass spectrometry (ICP-MS).[13] In addition, in the case of HeLa, A431, AML-12 and HT-29 cells, it is clear that the PtNPs that penetrate into the cells are in the cytoplasm but no fluorescence is observed in the nuclei (Figure 2, right column). In the case of HepG2, fluorescence is observed uniformly across the cell (Figure 2). Based on these findings, we proposed that the fluorescence in the nuclei in HepG2 cells originates either from a partial translocation of PtNPs into the nucleus or from oxidation of the PtNPs in the cytoplasm by reactive oxygen species (ROS) that allow the formation of soluble Pt(II) species by the release of the peptide from the surface of PtNPs. These results were further supported by ICP-MS measurements.

Recovery of PtNPs from human blood serum

The extremely high affinity between avidin and biotin[24] has been widely used for many purposes, including in the development of purification and separation techniques. As we aimed at determining the stability of the PtNPs in biological environments such as human blood serum, the PtNPs were biotinylated in order to use the interaction between biotin and avidin for separating the PtNPs from a complex biological mixture.

PtNP-**1b** were incubated with human blood serum (HBS), for 48 h. Avidin-functionalized resin was then added to the mixture (SoftLink™ Soft Release Avidin Resin, Promega LTD; Figure 3b) and stirred for 3 h.

After applying a purification protocol that allows for the recovery of biotinylated PtNPs from the resin followed by dialysis, the sample was analyzed by TEM (Figure 3a), revealing

that the PtNPs were stable towards this process. No aggregation was observed and the morphology of the PtNPs remained virtually unchanged compared to the one observed before the experiment. The amount of Pt in the recovered sample was quantified by ICP-MS and compared to the amount of Pt before incubation with HBS. It was found that 58% of the Pt was recovered as PtNP-**1b**.

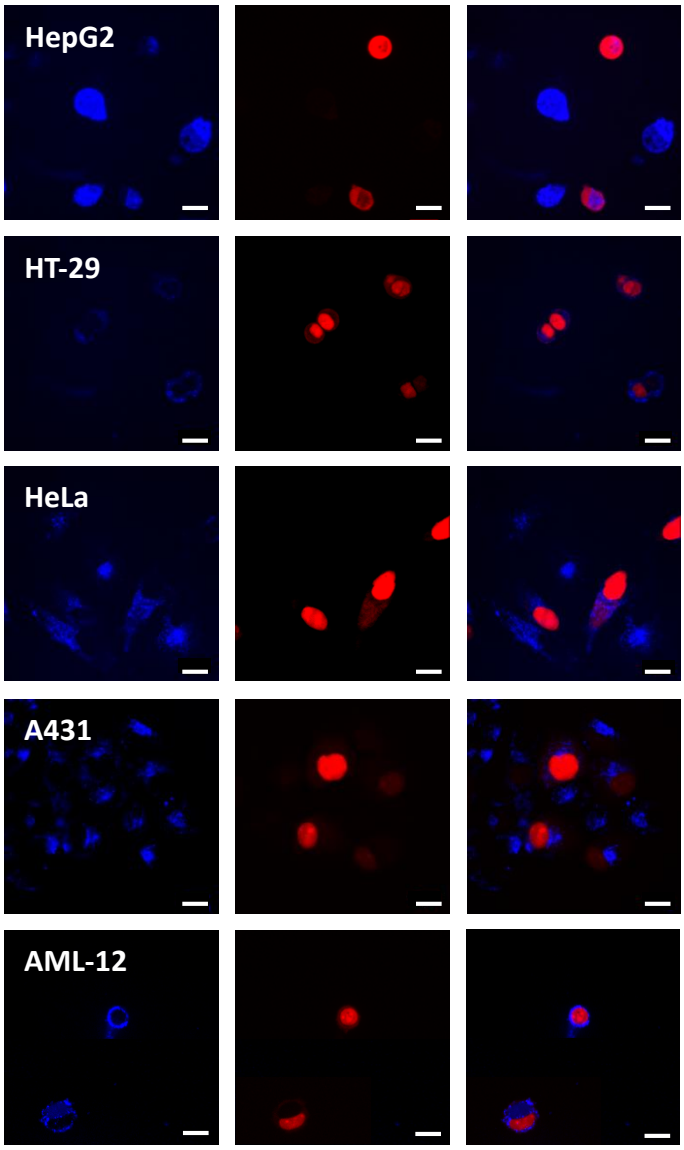

Figure 2. Confocal images of non-fixed cell-lines (HepG2, HT-29, HeLa, A431, and AML-12; incubated with the fluorescent labelled PtNP-**1a** at 2 mg/L for 12 h at 37 °C (left); counterstaining with nuclear marker CellLight™ Nucleus-RFP (middle) and superposition (right; scale bar 15 µm).

Enhancing cellular uptake

Post-reductive functionalization of the PtNPs-**1e2** that are decorated with an Arg residue allows for better cellular uptake, based on the well-investigated research on guanidinium-rich peptides as cell-penetrating vectors.[16-19]

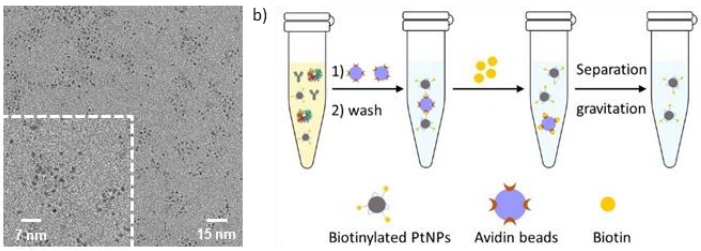

Figure 3. a) TEM micrograph of recovered PtNP-**1b** after 48 h in HBS. b) Schematic representation of PtNP recovery from HBS using biotin-avidin interactions.

To determine whether PtNP-**1e2** display improved cell penetrating properties with respect to the original system, a quantitative analysis of cellular uptake of PtNP-**1e** and PtNP-**1e2** in HepG2 cells was performed by ICP-MS. For that purpose, the cells were incubated with the PtNPs for 12 h, and then extensively washed in order to remove any platinum that is not inside the cell. In addition, the cell-nuclei were isolated in several samples and further analyzed by ICP-MS in order to quantify the metal content in the nuclei. The lyophilized cells or cell nuclei were then digested and the amount of Pt was determined by ICP-MS (Table 2).

Table 2. Quantification of platinum inside cells by ICP-MS

			[Pt] / ng/mg[a]	
Entry	Cell-line	PtNP-**1**[13]	PtNP-**1e**	PtNP-**1e2**
	Whole cells[b]			
1	HepG2	40 ± 1	40 ± 15	81 ± 14
2	HT-29	19 ± 5	14 ± 4	30 ± 7
	Nuclei[c]			
3	HepG2	29 ± 5 (72%)	24 ± 4 (60%)	36 ± 4 (44%)
4	HT-29	5 ± 3 (26%)	3 ± 1 (21%)	3 ± 1 (10%)

[a] Pt amount: Pt ng / cells mg, as the mean ± standard deviation of at least three repeats. [b] Pt amount in whole cells. [c] Pt amount in the nuclei; percentage of the total amount of Pt listed in brackets.

The amount of Pt that was found in the whole cells after incubation with PtNP-**1e2** was 63.1 ng/mg cells which is 1.7 times higher than the amount found after incubation with PtNP-**1e** (36.8 ng/mg). The amount of Pt that was detected in the isolated nuclei upon incubation with PtNP-**1e2** was 1.9 times higher compared to PtNP-**1e**, suggesting that the guanidinium group improves not only the cellular uptake but also increases the rate of nuclei translocation.

The effect of PtNP-**1e2** on the viability of the human hepatocellular carcinoma cells (HepG2) was then examined and was compared to the results obtained for PtNP-**1e** and PtNP-**1**. The PtNPs were added to the cells and incubated for 3 days before cell viability was determined by MTT assay.[25] The IC_{50} value and the maximal inhibition of PtNP-**1e** were 2.8 ± 0.2 mg/L and 79%, respectively (Figure 4). PtNP-**1e** inhibited the cell-viability similarly to PtNP-**1** (2.9 ± 0.3 mg/L and 79%), indicating a negligible effect of the azide group on the biological properties of the PtNPs. PtNP-**1e2** on the other hand, inhibited the cell viability more significantly, with maximal inhibition of 90%. This finding supports that positive charges on the surface of the NP

increase their cellular uptake and therefore improve the cytotoxic effect.

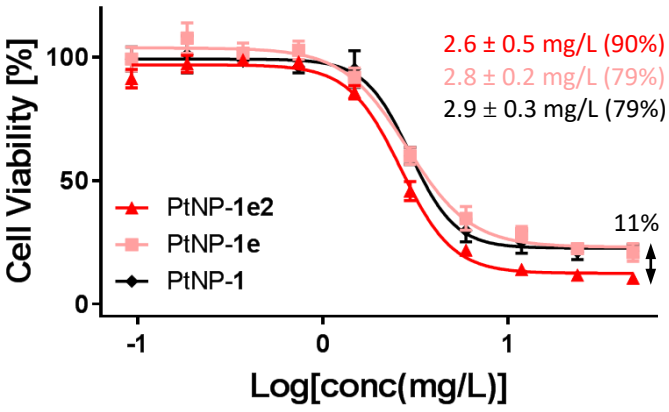

Figure 4. Dependence of HepG2 cell viability on administrated concentration of PtNP-**1** (black), PtNP-**1e** (light red) and PtNP-**1e2** (red).

Conclusions

We developed a peptidic system that not only enables the formation and stabilization of small and monodisperse PtNPs in water but also enables their covalent surface modification. All neutral moieties that were attached to the peptide (glucose, coumarin and biotin) showed no effect on the formation of the PtNPs. The system is intolerant to pre-reductive functionalization with positively charged moieties, and any attempt to form PtNPs using these peptide analogues failed. We believe that one or both of the following reasons cause the destabilization: electrostatic repulsion between the Pt(II) ions and the peptide before addition of the reducing agent in the NP formation process, or a binding competition between the guanidinium group and the Lys side chains which interrupts the packing of the peptide on the surface. To enable introduction of such moieties into the peptide, metal-free Staudinger-Bertozzi ligation that allows for formation of a strong covalent bond between the reaction partners and can be easily monitored by ^{31}P NMR. Overall, these results reveal the wide scope that our peptide-coated PtNPs can be functionalized with and used for.

Conflicts of interest

There are no conflicts to declare.

Acknowledgements

This project has received funding from the European Union's Horizon 2020 research and innovation programme under the Marie Sklodowska-Curie grant agreement No 705970. We are grateful to Leyla Hernandez for assistance in cell culture. We thank the Scientific Center for Optical and Electron Microscopy (ScopeM) for access to high resolution TEM and confocal microscope. We also thank Dr. Bodo Hattendorf and Prof. Detlef Günther (ETH Zurich) for access to ICP-MS instruments.

Notes and references

1. M. B. Dickerson, K. H. Sandhage and R. R. Naik, *Chem. Rev.*, 2008, **108**, 4935-4978.
2. C. L. Chen and N. L. Rosi, *Angew. Chem. Int. Ed.*, 2010, **49**, 1924-1942.
3. S. Eckhardt, P. S. Brunetto, J. Gagnon, M. Priebe, B. Giese and K. M. Fromm, *Chem. Rev.*, 2013, **113**, 4708-4754.
4. S. Corra, M. S. Shoshan and H. Wennemers, *Curr. Opin. Chem. Biol.*, 2017, **40**, 138-144.
5. J. Conde, G. Doria and P. Baptista, *J. Drug Deliv.*, 2012.
6. G. Doria, J. Conde, B. Veigas, L. Giestas, C. Almeida, M. Assunção, J. Rosa and P. V. Baptista, *Sensors*, 2012, **12**, 1657.
7. R. R. Arvizo, S. Bhattacharyya, R. A. Kudgus, K. Giri, R. Bhattacharya and P. Mukherjee, *Chem. Soc. Rev.*, 2012, **41**, 2943-2970.
8. M. A. Neouze and U. Schubert, *Monatsh. Chem.*, 2008, **139**, 183-195.
9. R. Subbiah, M. Veerapandian and K. S. Yun, *Curr. Med. Chem.*, 2010, **17**, 4559-4577.
10. R. A. Sperling and W. J. Parak, *Philos. Trans. Royal Soc. A*, 2010, **368**, 1333-1383.
11. H. Heinz, C. Pramanik, O. Heinz, Y. Ding, R. K. Mishra, D. Marchon, R. J. Flatt, I. Estrela-Lopis, J. Llop, S. Moya and R. F. Ziolo, *Surface Sci. Rep.*, 2017, **72**, 1-58.
12. C. Wilhelm, C. Billotey, J. Roger, J. N. Pons, J. C. Bacri and F. Gazeau, *Biomaterials*, 2003, **24**, 1001-1011.
13. M. S. Shoshan, T. Vonderach, B. Hattendorf, H. Wennemers, *Angew. Chem. Int. Ed.*, 2019, **58**, 4901-4905.
14. Functionalization of Pro5 affected the stability of the PtNPs, indicating that at this residue bulky moieties interfere with the assembly.
15. E. Saxon and C. R. Bertozzi, *Science*, 2000, **287**, 2007-2010.
16. Y. A. Nagel, P. S. Raschle and H. Wennemers, *Angew. Chem. Int. Ed.*, 2017, **56**, 122-126.
17. M. Green and P. M. Loewenstein, *Cell*, 1988, **55**, 1179-1188.
18. A. D. Frankel and C. O. Pabo, *Cell*, 1988, **55**, 1189-1193.
19. D. Kalafatovic and E. Giralt, *Molecules*, 2017, **22**.
20. P. Gobbo, W. Luo, S. J. Cho, X. X. Wang, M. C. Biesinger, R. H. E. Hudson and M. S. Workentin, *Org. Biomol. Chem.*, 2015, **13**, 4605-4612.
21. R. Arcos-Ramos, M. Maldonado-Dominguez, J. Ordonez-Hernandez, M. Romero-Avila, N. Farfan and M. D. Carreon-Castro, *J. Mol. Struct.*, 2017, **1130**, 914-921.
22. See supporting informaion for more details.
23. This time-frame of 12 hours was chosen since no PtNP toxicity was obsereved at this time.
24. O. H. Laitinen, V. P. Hytönen, H. R. Nordlund and M. S. Kulomaa, *Cell. Mol. Life Sci*, 2006, **63**, 2992-3017.
25. N. Ganot, S. Meker, L. Reytman, A. Tzubery and E. Y. Tshuva, *J. Vis. Exp.*, 2013, **81**, e50767.